Experimental Impact of Power Re-Optimization in a Mesh Network

Xin Yang[1,2,*], Alessio Ferrari[1], Dylan Le Gac[1], Gabriel Charlet[1], Massimo Tornatore[2], Yvan Pointurier[1]

[1]*Huawei Tech. France, Paris Research Center, Optical Comm. Tech. Lab*
[2]*Politecnico di Milano*
**Corresponding author: xin.yang@polimi.it*

Received XX Month XXXX; revised XX Month, XXXX; accepted XX Month XXXX; posted XX Month XXXX (Doc. ID XXXXX); published XX Month XXXX

We experimentally observe the SNR degradation of previously established services induced by loading new services in a network, and mitigate this degradation by periodic power re-optimization via 2 different strategies: 1) a static strategy based on end-of-life parameters, and 2) a dynamic strategy based on real-time monitoring to the current state of the network. We use a mesh network testbed of 4 nodes and 5 links with commercial equipment only. We observe up to 3.4 dB SNR degradation on the previously established services due to the loading of new services. Then we demonstrate an improvement of up to 3.2 dB in the network margin achieved by applying our proposed power re-optimization strategy. ©2022 The Author(s)

http://dx.doi.org/10.1364/JOCN.99.099999

1. INTRODUCTION

With the advent of the globalized information age, people's reliance on Internet services has increased dramatically. Optical fiber networks are used as Internet backbone, and have evolved vastly over the past decades through techniques such as Wavelength Division Multiplexing (WDM), advanced optical digital signal processing, improved fiber design and manufacturing, advances in optical amplifiers, etc. Recently, with the emergence of 5G (and soon 6G) services, new communication patterns driven by services in new areas as Internet of Thing (IoT), smart homes, unmanned smart driving, etc. [1] are appearing in backbone networks, and they will bring new practical challenges to current optical networks. New more robust and larger-capacity optical networks are urgently needed to meet growing needs of these new services.

High Quality of Transmission (QoT), such as low Bit Error Rate (BER) or high Signal-to-Noise Ratio (SNR), of services in optical networks is key to ensure large capacity and robustness of services in an optical network. Services in optical networks co-propagate, over different wavelengths, with other services through one or several links or Optical Multiplex Sections (OMSes); hence, services' SNRs can be impacted by many load-dependent physical effects such as Kerr effect (i.e. Self-Phase Modulation (SPM), Cross-Phase Modulation (XPM), Four-Wave Mixing (FWM)), Stimulated Raman Scattering (SRS), Wavelength Dependent Loss (WDL), and load-dependent gain spectrum of Erbium-Doped Fiber Amplifiers' (EDFA), thus the Amplified Spontaneous Emission (ASE) noise. These load-dependent effects make SNR of established services vary upon load changes, e.g. upon new services establishment or dropping, or simply upon power variations of the established services. SNR variations induced by load change may cause the service QoT to decrease below the SNR that corresponds to the Forward Error Correction (FEC) threshold, thereby causing outages.

To avoid service disruption in the cases described above, network designers are posed with the challenge to allocate enough design margins at network design time. In fact, reducing overall design margins, while making sure that the SNR margin of the service closest to FEC limit is maximized, can translate into increasing operation margins, which makes networks more robust to aging (e.g., due to fiber attenuation increase caused by fiber splices), or increase the capacity of optical networks, longer networks' life, and less deployment cost (CAPEX) or total cost of ownership during networks' life [2].

When accomodating new services into the network, certain operators prefer using the so-called "set and forget" operation mode [3,4,5] to set their powers. In "set and forget" mode, powers of new services are set using a pre-defined rule (e.g., powers are optimized for a fully loaded network); while, the powers of previously established services are not touched, thereby their powers, hence their SNRs, are left to drift without being adjusted to the new network state.

To maintain services running at their optimum SNR, powers of all services, both previous and new, can be re-optimized with different strategies upon any network layer change. Power re-optimization strategy (or "power re-equalization") consists of allocating power to each service by properly actuating the per-channel attenuation of the Wavelength Selective Switch (WSS) at the beginning of each OMS [9,10]. Through power re-optimization, the SNR of the worst service can be maintained at its optimum level, which helps to decrease design margin and increase operation margins. However, it has also to be taken into account that, providing a reliable dynamic solution is challenging as the

transient of the devices has to be kept under control, also the scalability of the solution as well as the time required by the devices to converge to the new configuration. Some of these issues are, for instance, addressed in [6].

This paper is an extended version of our ECOC 2022 paper [11]. The aim of this paper is two-fold. First, we experimentally quantify the SNR degradation of previously established services as new services are established in a realistic mesh network. Second, we experimentally quantify and compare the network margin improvement of both previously established and new services when using two existing power re-optimization strategies.

In this experiment work, our mesh network testbed consists of 4 nodes and 5 OMSes with heterogeneous span type and length built with only commercial equipment that would be deployed at operators', and up to 292 services are established. Our experiment demonstate SNR variations due to load change of several dBs, which can be fully recovered through proper power re-optimization strategies. We also show good match between the predicted SNR (that we obtained using a digital twin) and the measured SNR after power re-optimization, which ensures good reliability of applying power re-optimization strategies.

The remainder of the paper is structured as follows. In Section 2, we introduce two power optimization strategies to mitigate SNR degradation due to loading new services in the network. In Section 3, we introduce the network loading scenario where procedures of services' loading and power re-optimization are described. In Section 4, we introduce our 5-OMS mesh network testbed. In Section 5, we experimentally evaluate the SNR degradation induced by loading new services, and the SNR improvement by applying power re-optimization strategies.

2. POWER OPTIMIZATION STRATEGIES

In this section, we define two different power optimization strategies, 1) a static End-of-Life design strategy (static strategy) and 2) a dynamic real-time strategy (dynamic strategy), to mitigate SNR degradation of previously established services caused by loading new services in the network. These power optimization techniques are implemented by setting the per-channel launch output power at the first ("booster") amplifier of each OMS in a network.

A. Static End-of-life (EoL) design strategy

The first strategy is based on a "static" End-of-Life (EoL) design strategy, which consists in computing the launch power based on EoL assumptions, therefore, it never changes during network lifetime. To set the EoL launch power, only "static" parameters are used. These parameters can be obtained at the design stage or at the initial commissioning of the network at Beginning of Life (BoL) (see Tab. 1), namely, fiber length, fiber type, span loss, and estimated connector loss. This static EoL strategy sets the launch power based on the Local-Optimum Global-Optimum (LOGO) formula [7], that assumes Full Spectral Load (FSL). LOGO aims at optimizing SNR of the worst channel at OMS level by providing a flat power allocation (P_{LOGO}) as input power into the fiber for each span by means of the analytical formula:

$$P_{LOGO} = \sqrt[3]{\frac{P_{ASE}}{2\eta}}. \quad (1)$$

P_{LOGO} is derived under the assumptions of flat power spectrum, flat amplifier gain spectrum, flat fiber attenuation, and the SRS effect is not taken into account. P_{ASE} is the ASE noise power generated by the EDFA and η is the nonlinear efficiency evaluated under FSL assumption.

Since static, BoL parameters are used for this power re-optimization throughout the network life, until EoL, this strategy is suboptimal.

B. Dynamic real-time strategy

The "dynamic" real-time strategy also aims at optimizing the SNR of the worst channel at each OMS, but in a dynamic fashion. The optimal launch power provided by the dynamic strategy is calculated based on Gaussian noise (GN) model [7,8] considering wavelength-dependent gain spectrum, wavelength dependent fiber attenuation, and the SRS effect so that the power ratio of ASE noise to nonlinearity is 3 dB for each channel at OMS level [9,12]. The dynamic strategy requires not only "static" parameters, but also real-time parameters obtained from the monitoring of the network, either directly (output power spectrum of the first and last amplifiers at each OMS, total input and output powers at each amplifier) or indirectly through parameters refinement (connector losses, gain spectra, power spectra of the in-line amplifiers) [13]. This strategy relies on real-time monitoring of the network, therefore, it can provide dynamic changes to the network state. The optimal power per channel at the booster of each OMS has been computed and adjusted with current network configuration to attain the heuristic rule targeting 3 dB for the ASE noise to non-linear power ratio for each channel at each OMS similarly to [9,12].

In the following results, we observe that this dynamic power re-optimization strategy outperforms the static strategy thanks to the feedback of real-time monitoring.

TAB. 1 Required parameters for power re-optimization.

"Static" parameters (design and commissioning)	"Dynamic" parameters (real-time monitoring)
fiber type; fiber length; span loss; connector loss (estimated)	total input and output powers at each amplifier; output power spectrum at WSS sides at each OMS; gain, power profiles of the in-line amplifiers (estimated)

3. NETWORK LOADING SCENARIO

We consider a mesh optical network where we progressively load services and periodically apply power re-optimization for all the existing (previous and new-loaded) services. Sources and destinations of services are randomly picked among network nodes. Without loss of

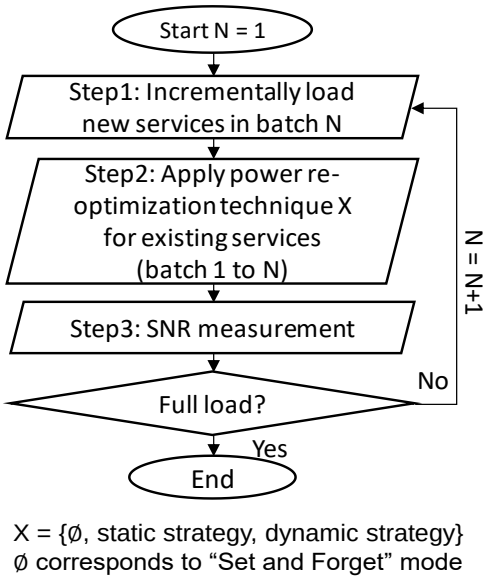

Fig. 1 Flowchart of the experiment.

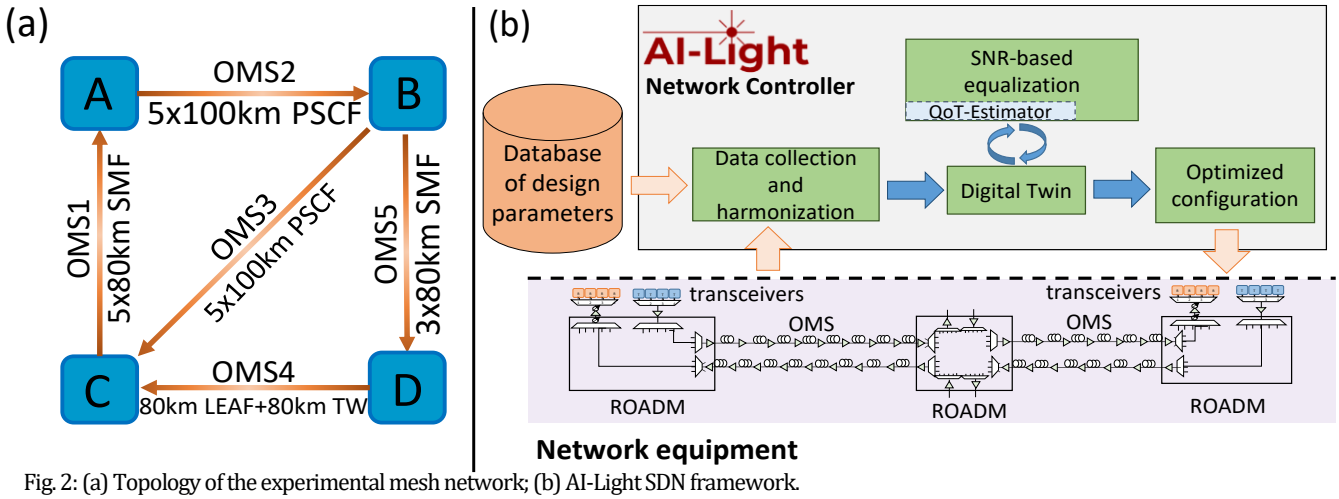

Fig. 2: (a) Topology of the experimental mesh network; (b) AI-Light SDN framework.

generality of our results, we assume service route is selected using a shortest path routing algorithm, and we apply a first-fit wavelength assignment to load services from long to short wavelength in the network. If a service is blocked due to lack of resources, we simply select a new demand, until the full load is achieved. The flowchart of the experiment is shown in Fig. 1.

For each services batch N:

- Sequentially establish each new service of batch N and set its launch power for each crossed OMS with the static EoL design power (P_{LOGO}) (Section 2-A); We do not re-optimize previous services from the same batch in this step;
- Once all services of one batch are loaded, apply power re-optimization strategy on all existing (previous and new) services with either: a) "set and forget" (i.e., do nothing), b) static power strategy (Section 2-A) or c) dynamic power strategy (Section 2-B);
- Measure SNRs of all existing services in the network;
- Repeat with next batch N+1 until network becomes fully loaded.

Note that with "set and forget" mode, the launch power of each new service is set as P_{LOGO}, but never re-optimized regardless of power drift induced by loading new services in the network.

4. EXPERIMENTAL TESTBED

We experimentally implement in our lab a mesh network with 4 nodes (A, B, C, D), 5 (unidirectional) OMSes, whose topology is depicted in Fig. 2(a). Tab. 2 shows the routing table of 12 paths with corresponding source node, sink node, crossed OMS, and path lengths. Span informations such as span number, fiber type, fiber length of each OMS are shown both in Fig. 2(a) and Tab. 3. Since the traffic demand is increasing exponentially in recent years, we emulate exponential number of arrivals of new services by progressively loading 7 batches of services having size: 5, 5, 10, 20, 40, 80 and 132. Hence, over the time, the total number of services in the network will be 5, 10, 20, 40, 80, 160 and 292 after loading each new batch. In the experiment, the network is fully loaded when 292 services are loaded and all the wavelengths (80 channels of 75GHz on the 6THz C band) on all links are occupied.

Fig. 3(a) shows the allocation statistics for each batch; note that the maximum service length is 1140 km and the average service lengths in each batch are similar to service lengths in real typical large metro or small core networks.

TAB. 2 Routing table.

Source	Sink	Path	Length(km)
A	B	OMS2	500
A	C	OMS2-OMS3	1000
A	D	OMS2-OMS5	740
B	A	OMS3-OMS1	640
B	C	OMS3	500
B	D	OMS5	240
C	A	OMS1	400
C	B	OMS1-OMS2	900
C	D	OMS1-OMS2-OMS5	1140
D	A	OMS4-OMS1	560
D	B	OMS4-OMS1-OMS2	1060
D	C	OMS4	160

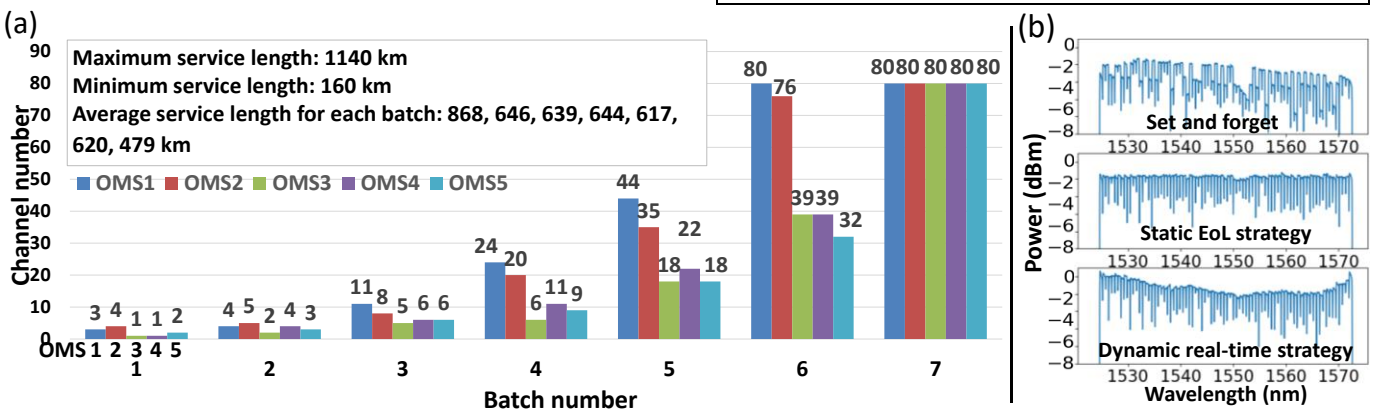

Fig. 3: (a) Number of services transported by each OMS after loading each batch; (b) Full-load normalized power spectrum at the output of the first EDFA of OMS1 with the "set and forget" operation mode, static strategy, and dynamic strategy.

TAB. 3 OMS per span information and corresponding P_{LOGO}.

	OMS1	OMS2	OMS3	OMS4	OMS5
Spans	5x80km SMF	5x100km PSCF		80km LEAF+80km TW	3x80km SMF
P_{LOGO} (dBm)	[2.9, 4.1, 2.2, 1.9, 3.1]	[5.1, 4.7, 6.7, 4.4, 6.0]	[4.5, 4.6, 6.1, 4.5, 5.4]	[0.8, 1.2]	[3.1, 4.4, 3.0]

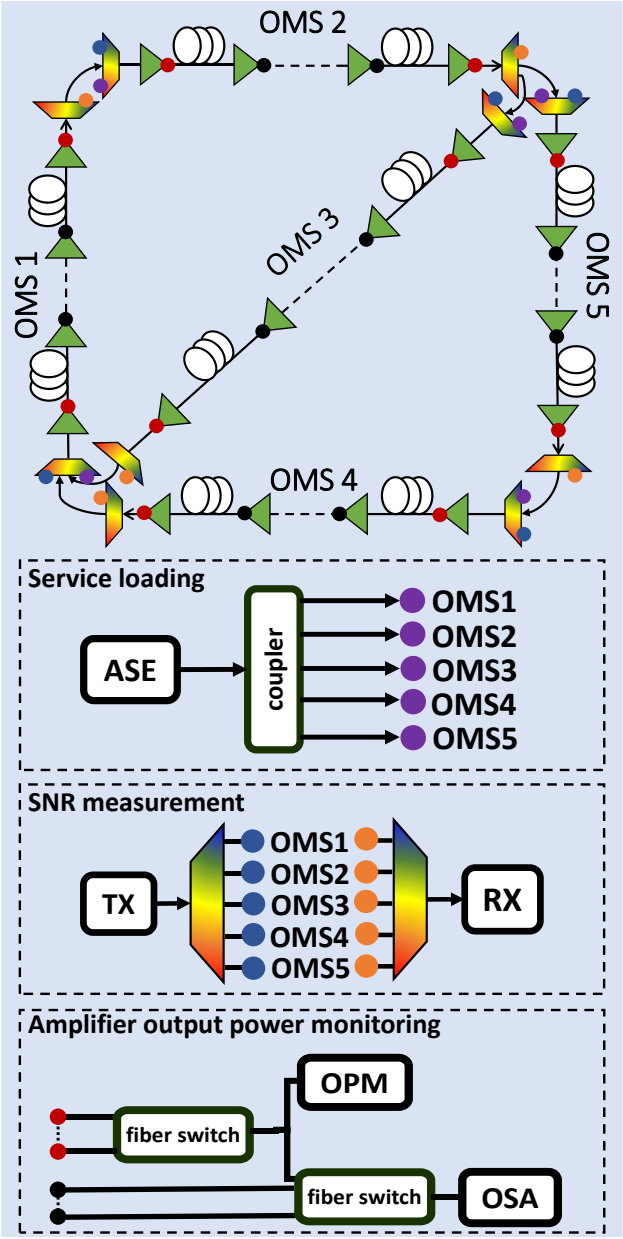

Fig. 4: Experimental testbed with details about service loading by ASE source, SNR measurement by transponder, and output power monitoring by OPM (OSA is for results analysis).

Fig. 4 shows some further details of the experimental testbed. Only commercial equipment is used to implement the network. The transmitter (TX) of the transponder is connected to a WSS whose ports are connected to each OMS (blue dots shown in Fig. 4). Then the egress of each OMS is connected to a port of a WSS (orange dots shown in Fig. 4) which is connected to the receiver (RX) of the transponder. Such architecture is used to automate the SNR measurement of different paths in the network. The real-time commercial transponder generates a Polarization-Division-Multiplexed QPSK signal with 68Gbaud baud rate, 200 Gb/s bit rate with 75GHz channel spacing. In addtion, we rely on an ASE source when we progressively load the network to emulate all the services that are allocated in the network. ASE source is connected using a coupler to each OMS (purple dots shown in Fig. 4). The launch power of these *dummy* services is set at the targeted value computed by power optimization strategies, i.e., static or dynamic strategy. Then, we measure the SNR of each service by sequentially replacing each *dummy* service with the signal generated from the commercial transponder. We measure the pre-FEC BER and we apply the back-to-back curve of the transponder to obtain the measured SNR as shown in [14]. ASE source is the only part in the experiment that does not rely on commercial equipment. To monitor power spectrums, we use an Optical Power Meters (OPM) and Optical Spectrum Analyzer (OSA). Power monitoring points are marked as red (by OPM or OSA) and black (by OSA). OPM is a commercial product that monitors the per-channel output power at the first and last amplifier of each OMS, as in a real network, rather than a lab-grade OSA (an OPM is a low-cost OSA with lower accuracy), while OSA monitors the output power spectrum of each amplfier, however, it is not involved in the optimization process nor in the configuration of the network. The OSA has been only used to better observe and analyze results. All monitoring points are connected with fiber switches so that the power spectrum of interest can be switched and monitored. Optical amplifiers and WSSes are also commercial products. Unless otherwise stated, we use only information available in real networks such as total input/output power monitored by photodiodes at each amplifier, output power spectrum at the first and last amplifier of each OMS (with an OPM as explained above), fiber length and fiber type of each span. In addition, to save time, we measured the SNR values of only odd-indexed services, hence half of the services. Without loss of generality, we report SNR margin which is defined as:

$$SNR\ margin = SNR_{monitored} - SNR_{FEC} \quad (2)$$

where $SNR_{monitored}$ is the monitored SNR by the real-time transponder and SNR_{FEC} is the minimum sufficient SNR that service needs for a successful transmission, which corresponds to FEC threshold.

Fig. 2(b) summarizes the relation among service management, real-time monitoring, data collection, GN-model based SNR estimation and power re-optimization with our Autonomous Driving Network "AI-Light" Software Defined Networking (SDN) platform described in [14], which implements a digital twin. Our digital twin works similarly as GNPy [15], and we leverage it to compute optimal launch power of the dynamic power optimization strategy (Section 2-B) considering all load-dependent effects as described in Section 1, and also non-load-dependent effects such as WSS filtering and transponder back-to-back noise. The validation of our digital twin is shown in Section 5-C.

Tab. 3 shows the computed P_{LOGO} per span per OMS based on the "static" parameters. Note that P_{LOGO} of each span is also used to configure amplifiers's gain and tilt so that their output power matches the one provided by the LOGO. Notably, amplifier configurations are set at the beginning of the experiment and never reconfigured. Fig. 3(b) shows examples of full load output power spectrum captured by an OSA at the

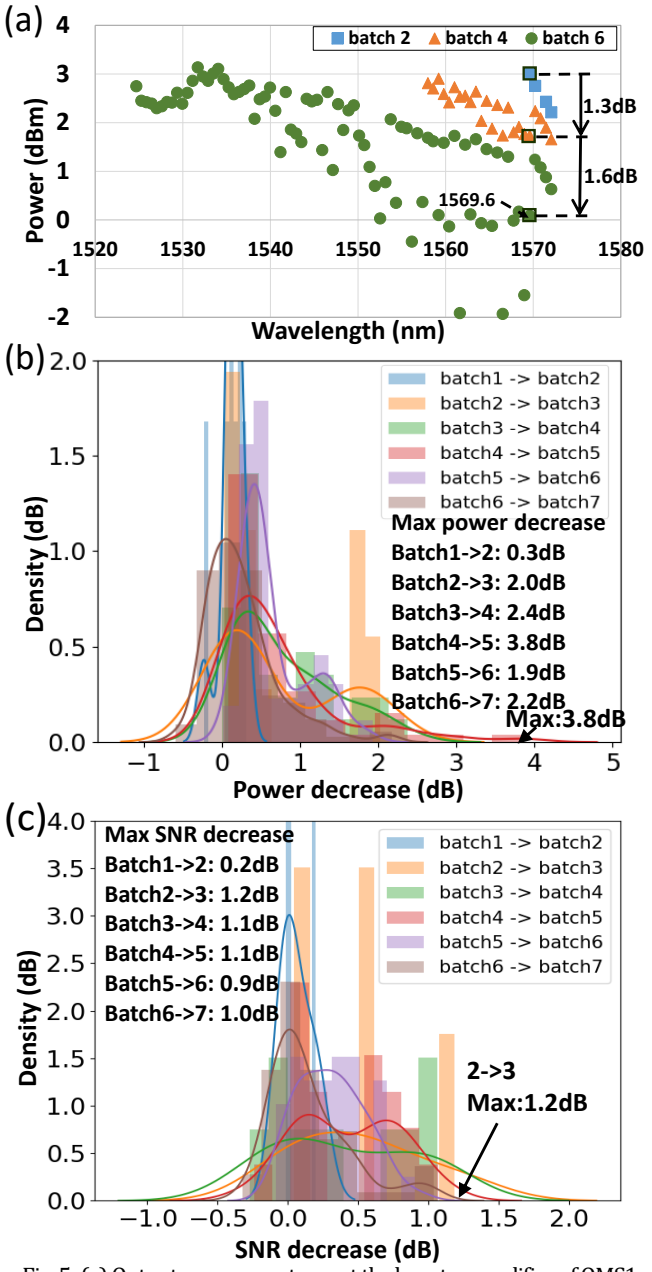

Fig. 5: (a) Output power spectrum at the booster amplifier of OMS1 after loading batch 2/4/6; (b) Power decrease at the booster amplifier on each OMS of previously existing channels (batch N) due to loading new batch of services (batch N+1); (c) SNR decrease of existing services (batch N) due to loading new services (batch N+1).

first EDFA on OMS1 when the network is fully loaded. Each subplot shows the power spectrum for each power optimization strategy: "set and forget" (top), static (middle), and dynamic (bottom), highlighting the sharp differences in power allocation across different strategies.

5. RESULTS

In this section, first we report results of channel power, gain variation, and SNR degradation of the previously established services induced by loading new batches of services (Section 5-A and Figs. 5, 6). Second, we show the SNR improvement by periodically applying both a static or a dynamic power strategy (Section 5-B and Fig 7). Finally, in Section 5-C and Fig. 8 , we compare the predicted SNR vs. monitored SNR after the power re-optimization with static or dynamic strategy, showing that the expected SNRs predicted by our digital twin fit well the reality, demontrating the feasibility and reliability of the re-optimization.

A. SNR degradation by loading new services

Fig. 5(a) shows the output power spectrum measured at the first amplifier on OMS1 after loading different batches of services with the "set and forget" operation mode. After loading batch 2/4/6 respectively, the number of established channels on OMS1 are 4/24/80 (see Fig. 3(a)). We observe that the power of a sample service (with wavelength 1569.6 nm) decreases by 1.3 dB after 24 channels are established on OMS1 (batch 2 → 4), then, the power of the same service decreases by an additional 1.6 dB after all 80 channels are loaded (full load) on OMS1 (batch 2 → 6).

Statistical results of the power variation is shown in Fig. 5(b), which depicts the Probability Density Function (PDF) and maximum values of channel power decrease of existing channels in batch N induced by loading new services in batch N+1. The power is monitored at the output of the booster amplifier on each OMS. We observe that the maximum power drop induced by loading new batches reaches 3.8 dB for N = 4. The booster power variation is caused by both the load-dependent SRS variation and the gain spectrum variation due to loading new services. This shows that the power can drift dramatically with different load states in the network, which can cause SNR degradation, as described next.

Fig. 5(c) shows the PDF and maximum values of SNR degradation of previously established services in batch N impacted by loading new services in batch N+1. We observe that the maximum SNR decrease after loading new batches is up to 1.2 dB for N = 2. This SNR decrease of previously established services induced by loading new services warrants the great importance of applying power re-optimization strategy not only of new added services, but also of previously established services to avoid large SNR decrease, hence disruption of service when loading new services.

To further study the impact of loading new services, we focus on the first-loaded service ("Service #1").

In Fig. 6(a), the blue line shows the SNR degradation of Service #1 after sequentially loading each batch of services when applying "set and forget". Service #1 goes through OMS 1-2-5, crossing 13 heterogeneous spans and 16 EDFAs with service length of 1160km. We observe that SNR of Service #1 starts to sharply drop by 1.2 dB after loading 3 batches of 20 services in the network and decreases by up to 3.4 dB after loading 7 batches of all 292 services, at which point the network is fully loaded.

To further study the SNR degradation caused by the load-dependence of EDFA gain profile, we track the variation of channel gain (Fig. 6(b)) and channel output power (Fig. 6(c)) with OSA along each EDFA that Service #1 crosses as different number of batches of services are loaded in the network. In Fig. 6(b), we observe that the channel gains of EDFAs crossed by Service #1 generally decrease as new services are loaded in the network (as ripples are load-dependent, it is possible that the power of some services increase as well). After loading all 292 services (batch 7), the maximum and average channel gain decrease are respectively 1.3 and 1.1 dB among all the crossed EDFAs. The channel gain variation induced by the load-dependence of the gain spectrum contributes to channel power variation, as shown in Fig. 6(c). In Fig. 6(c), we can observe that the channel output power measured at the end of transmission of Service #1 decreases by up to 6.6 dB when all 292 services are loaded in the network, which corresponds to up to 3.4 dB SNR drop in Fig. 6(a). We can also observe that the power decrease is roughly proportional to the number of crossed amplifiers due to the accumulation of gain variation induced by load-dependent gain profile

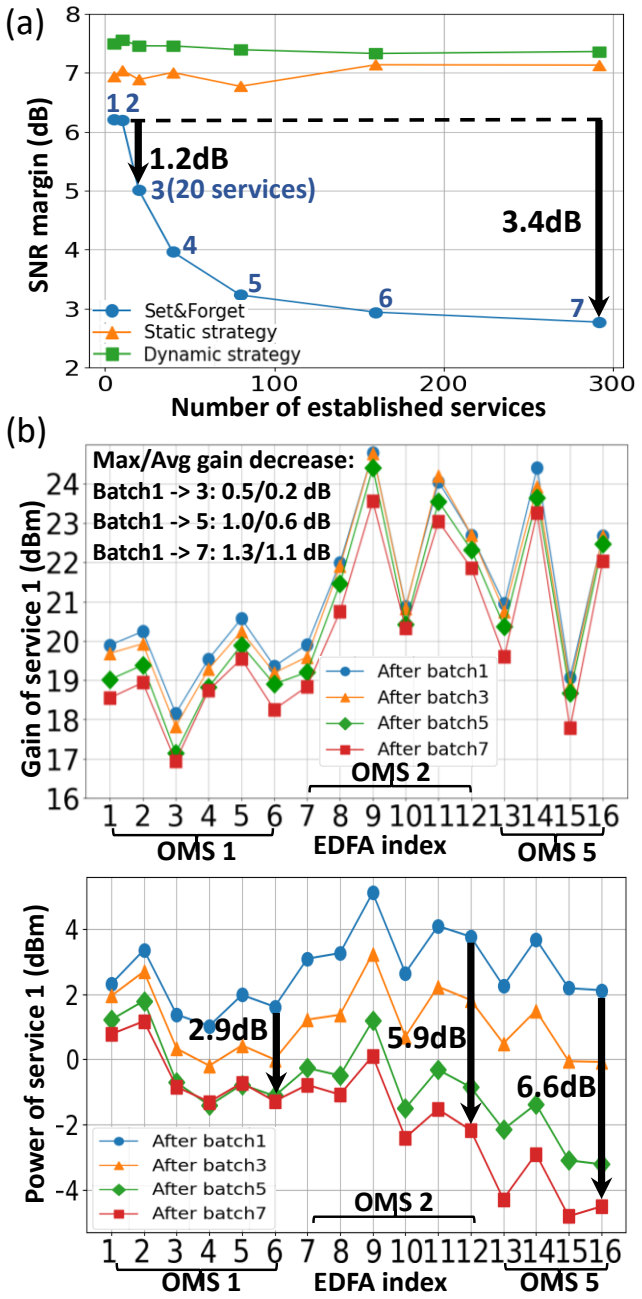

Fig. 6: (a) SNR variation of Service #1 with different number of established services; (b) Gain of Service #1 at each traversed EDFA; (c) Power of Service #1 after each traversed EDFA.

of each EDFA. In Fig. 6(c), we observe 2.9/5.9/6.6 dB power decrease at the last EDFA of OMS 1/2/5 after loading all 292 services in the network. This could be also observed in Fig. 3(b), where the power spectrum was measured at the output of the first EDFA of OMS 1 with "set and forget" mode, shows roughly 3 different power levels due to different number of EDFAs that services cross before arriving to the first EDFA on OMS 1, and the lower channel powers correspond to larger power decreases, i.e., to services that cross more EDFAs, hence more OMSes.

Applying periodic power re-optimization strategy such as static strategy (in orange) or dynamic strategy (in green) in Fig. 6(a) mitigates the SNR degradation induced by loading new services. In Fig. 6(a), we can observe that SNR margin of the Service #1 can always be maintained at a high level after loading each batch of services until full load is reached. Indeed, for the Service #1, SNR margins are always improved of at least 6.5 dB when loading different number of services by applying the static strategy, and more than 7dB SNR margins is always achieved by the dynamic strategy. In addition, we can observe that SNR margins of the Service #1 are always higher with the dynamic strategy compared with the static strategy after each batch loading (e.g., in Fig. 6(a), green line is always above orange line). This is due to the better launch power setting at each OMS by applying dynamic power re-optimization that is based on more accurate real-time monitoring during network life.

B. SNR improvement by power re-optimization strategies

Fig. 7(a) shows the SNR margin with static (circle) or dynamic (triangle) power re-optimization strategy vs. "set and forget" mode of operation after loading new batches of services. The diagonal black line shown in Fig. 7(a) corresponds to the situation where the power re-optimization does not improve/degrade SNR compared to "set and forget". Different colors correspond to different number of loaded services (after loading batch 1/4/7). We observe that most of the triangles and circles are above the black diagonal line, which means that most services' SNR margins with re-optimization strategies are larger than SNR margins with "set and forget" mode. Especially, after loading all 292 services in the network, the SNR margin of the service with the worst SNR improves by up to 4.6 dB with dynamic strategy. In addition, triangular markers are always above circle markers, which shows that dynamic strategy further improves SNR margins due to better adjustment to the actual monitored network configuration compared to the static strategy.

Fig. 7(b) shows the PDF of SNR margins of all 292 services when network is fully loaded for each power re-optimization strategy as well as "set and forget". Small SNR margins are all improved with both static and dynamic power re-optimization strategies. If we compare the smallest SNR margin among all services with and without power re-optimization, we observe in Fig. 7(b) that the smallest SNR margin is improved by 2.6 dB with the static strategy corresponding to A→C in Fig. 7(a) or 3.2 dB with the dynamic strategy corresponding to A→B in Fig. 7(a), where the smallest margin with "set and forget" is at point A, the margin with the dynamic strategy is at point B, and margin with the static strategy is at point C. This confirms that dynamic re-optimization strategy further improves SNR margin with respect to the static strategy thanks to real-time monitoring of network configuration.

Next, we study the correlation between SNR gain obtained by power re-optimization and the number of crossed OMSes. Fig. 7(c) shows the PDF of SNR gain of all existing services in the network after loading each batch (5, 10, 20, 40, 80, 160, 292 services are established in the network after loading each batch) when applying static (top) or dynamic (bottom) power re-optimization strategy compared to "set and forget" mode. Different colors correspond to SNR gain of services with different number of traversed OMSes. We can observe that after applying dynamic power re-optimization, the SNR decreases for a small number of services. This is because optimal launch power are not computed correctly mainly due to wrong estimation on back-to-back transponder penalty, which is highly transponder sample dependent especially for large SNR region [16,17]. Thereby, a small number of SNRs corresponding to services crossing single OMS are not improved and, in fact, it decreases by up to 0.9 dB or 0.8 dB with static and dynamic strategies respectively, however their margins remain still high. For services that cross 2 OMSes, their SNRs improve by up to 1.9 dB and average 0.3 dB with static strategy; up to 2.1 dB and average 0.5 dB with dynamic strategy. SNRs of certain services decrease slightly by 0.5dB and 0.3 dB with static and dynamic re-optimization respectively due to the same reason as described above. Finally, for services that cross 3

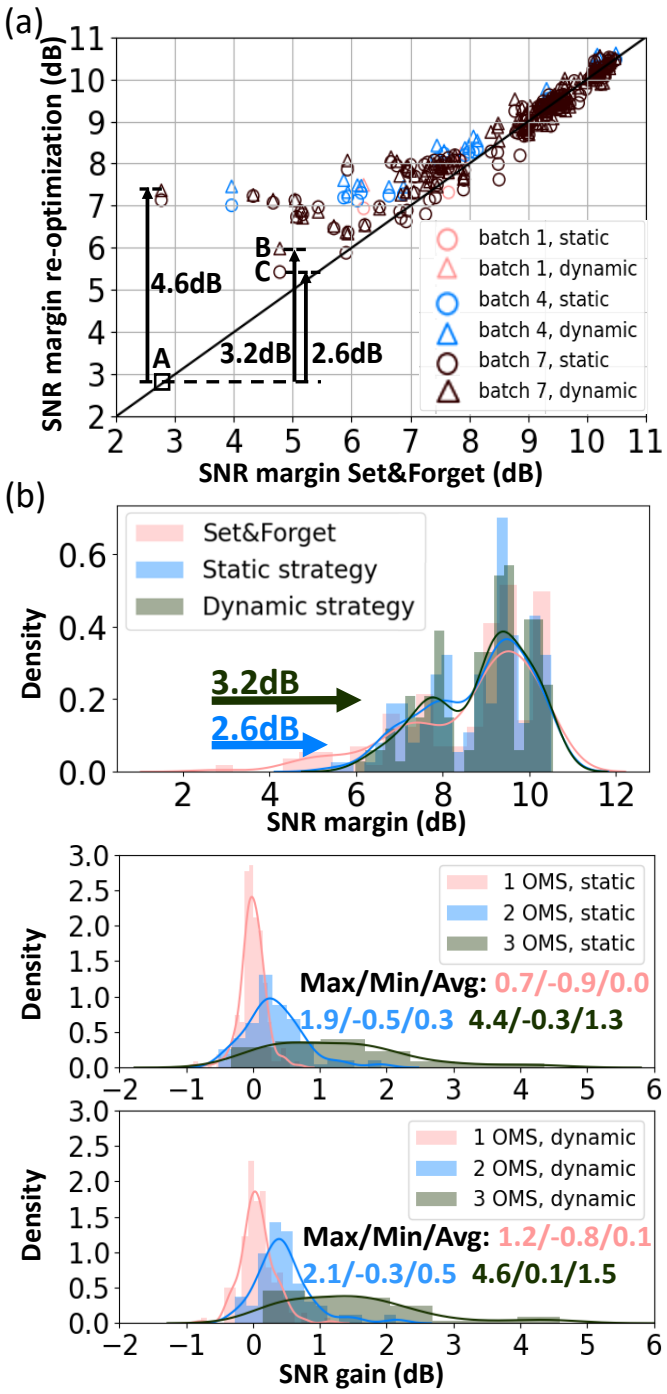

Fig. 7: (a) SNR of services with power re-optimization strategies vs. "set and forget"; (b) PDF of SNR margins; (c) PDF of SNR gain per length (1, 2, 3 OMS) and per power re-optimization strategy.

OMSes, SNRs are improved with both static and dynamic power re-optimization strategies. Dynamic power re-optimization strategy improves better SNRs for services with 3 OMSes compared to static power re-optimization strategy. The maximum improvement is 4.4 dB, and the average improvement is 1.3 dB by the static strategy, while maximum improvement is 4.6 dB, average improvement is 1.5dB by the dynamic strategy. Notably, the SNRs of the services that cross 3 OMSes are the smallest compared to services with 1 or 2 OMSes, however, these SNRs are always improved with dynamic power re-optimization strategy with a positive 0.1 dB minimum SNR improvement, average 1.5 dB SNR improvement, and maximum 4.6 dB improvement.

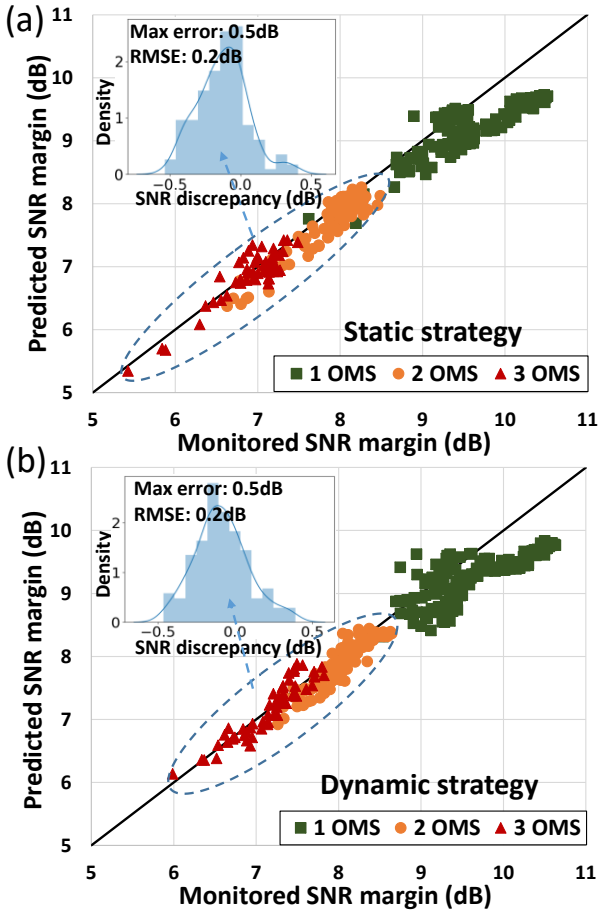

Fig. 8: Predicted SNR margin vs. measured SNR margin with (a) static strategy; (b) dynamic strategy.

C. Predicted SNR vs. monitored SNR with power re-optimization

Accurate QoT estimation/prediction by the digital twin is of key importance for accurate optimal launch power computation, ensuring that services can run at their optimum SNRs during network lifetime. In this section, we validate the accuracy of our digital twin by comparing the SNRs predicted by our digital twin using the optimal launch power computed at Step 1 of Fig. 1 vs. the monitored SNRs by the transponder after applying power re-optimization strategies, i.e., at Step 3. Since SNRs are predicted using the computed optimal launch power, the predicted SNRs are ones that we expect to achieve. Notably, only information available in real networks (see Tab. 1) is used for both launch power computation and SNR prediction.

In Fig. (8), we compare the predicted SNRs vs. monitored SNRs for both static (Fig. 8(a)) and dynamic (Fig. 8(b)) power re-optimization strategies after loading each batch of services. The diagonal black line shown in Fig. 8 corresponds to the hypothetical situation where SNRs monitored by the transponder are ideally predicted by the digital twin. As shown in both Figs. 8(a) and (b), SNRs are predicted more accurately for services with smaller SNRs which cross two (orange circles) or three OMSes (red triangles). All the services with large SNRs cross a single OMS (green squares), and they are mainly limited by transponder back-to-back noise, thereby their SNRs are predicted less accurately; however, SNR margins are still high for those services, so lower accuracy of prediction is still acceptable. Good prediction on small SNRs is more important because services with small SNRs have less margin,

hence easier to get disrupted due to wrongly predicted launch power setting. Inset PDF plots shows the SNR discrepancy between prediction and monitoring only for services that cross two and three OMSes (orange round points and red triangle points inside dashed blue circle). The maximum prediction error is 0.5 dB and the RMSE is 0.2 dB for both static and dynamic strategy, which can come from intrinsic QoT estimator error and inaccurate parameters estimation i.e., connector losses and gain/power spectra[i] of in-line amplifiers. The result shows that the predicted SNRs by our digital twin fits acceptably the monitored SNRs after applying power re-optimization strategy. Such accuracy of the digital twin during power re-optimization suggests that a feasible and reliable power re-optimization strategy can be applied in practice.

6. CONCLUSIONS

In this study, we experimentally quantify the impact of establishing new services on previously established services on a 5-OMS testbed using commercial equipment. We observe that SNRs of previously established services are decreased by up to 3.4 dB after loading close to 300 services in the network. To study SNR degradation due to loading new services in the network, we track the output power variation at each crossed EDFA of the first loaded service as example after loading different number of services in the network, and we find 6.6 dB power decrease at the end of transmission after propagating through 16 EDFAs. Then, we apply 2 different strategies, a static and a dynamic strategy, to mitigate the SNR degradation due to loading of new services in the network. We find that, using periodic per-service, per-OMS power re-optimization strategies, SNR margin is improved by up to 2.6 dB with static strategy that needs only "static" parameters that can be obtained from design and at commissioning, or 3.2 dB with a dynamic strategy that needs not only "static" but also "dynamic" real-time monitoring information. Both strategies improve significantly robustness of the network thanks to largely improved SNR margin of the worst service. Finally, we compare the predicted SNR and monitored SNR with applying static or dynamic power re-optimization strategy, and we find a good match between predicted and monitored SNR, which shows the optimized SNRs can be well predicted.

One limitation of this work is that we do not consider service dropping induced by fiber cuts. If a fiber cut happens, network load will change, which means we need to apply power re-optimization again for the OMSes traversed by the dropped services, which is time consuming. In the future, we may consider predicting power drift after loading new services in the network in order to reduce power re-optimization time to meet more practical requirements in real networks (e.g., power re-optimization including in fast re-routing to recover service caused by fiber cut with good SNR margin). Moreover, all the issues related to the scalability of the proposed strategy as well as the transient of the devices are critical aspects which we are planning to assess.

References

1. M.Z. Chowdhury, M. Shahjalal, M.K. Hasan and Y.M. Jang, "The Role of Optical Wireless Communication Technologies in 5G/6G and IoT Solutions: Prospects, Directions, and Challenges," Applied Sciences, vol. 9, no. 20, p. 4367, Oct. 2019.
2. Y. Pointurier, "Design of low-margin optical networks," J. Opt. Commun. Netw. 9, A9-A17 (2017).
3. P. Layec, A. Dupas, D. Verchère, K. Sparks and S. Bigo, "Will Metro Networks Be the Playground for (True) Elastic Optical Networks?," IEEE/OSA Journal of Lightwave Technology, vol. 35, no. 6, pp. 1260-1266, March 2017.
4. K. Christodoulopoulos, C. Delezoide, N. Sambo, A. Kretsis, I. Sartzetakis, A. Sgambelluri, N. Argyris, G. Kanakis, P. Giardina, G. Bernini, D. Roccato, A. Percelsi, R. Morro, H. Avramopoulos, P. Castoldi, P. Layec and S. Bigo, "Toward efficient, reliable, and autonomous optical networks: the ORCHESTRA solution [Invited],"IEEE/OSA J. Opt. Commun. Netw. 11, C10-C24 (2019).
5. J. Pesic, T. Zami and N. Rossi, "Cost savings for low design margins in WDM elastic networks," in Advanced Photonics, 2018, paper NeW3F.1.
6. Z. Zhong, M. Ghobadi, M. Balandat, S. Katti, A. Kazerouni, J. Leach, M. McKillop and Y. Zhang, "BOW: First Real-World Demonstration of a Bayesian Optimization System for Wavelength Reconfiguration," in Optical Fiber Communication Conference (OFC), 2021, paper F3B.1.
7. P. Poggiolini, G. Bosco, A. Carena, V. Curri, Y. Jiang and F. Forghieri, "The GN-Model of Fiber Non-Linear Propagation and its Applications," IEEE/OSA Journal of Lightwave Technology, vol. 32, no. 4, pp. 694-721, Feb. 2014.
8. D. Semrau, R. I. Killey and P. Bayvel, "The Gaussian Noise Model in the Presence of Inter-Channel Stimulated Raman Scattering," IEEE/OSA Journal of Lightwave Technology, vol. 36, no. 14, pp. 3046-3055, July 2018.
9. I. Roberts, J. M. Kahn and D. Boertjes, "Convex Channel Power Optimization in Nonlinear WDM Systems Using Gaussian Noise Model," IEEE/OSA Journal of Lightwave Technology, vol. 34, no. 13, pp. 3212-3222, 2016.
10. V. V. Garbhapu, A. Ferrari, I. F. de Jauregui Ruiz, D. Le Gac, G. Charlet and Y. Pointurier, "Network-Wide SNR-based Channel Power Optimization," in European Conference on Optical Communication (ECOC), 2021, paper Tu2E.5.
11. X. Yang, A. Ferrari, N. Morette, D. Le Gac, S. Escobar Landero, G. Charlet and Y. Pointurier, "Experimental Impact of Power Re-Optimization in a Mesh Network," in European Conference on Optical Communication (ECOC), 2022, paper Mo3B.3.
12. S. E. Landero, I. F. de Jauregui Ruiz, A. Ferrari, D. L. Gac, Y. Frignac and G. Charlet, "Link Power Optimization for S+C+L Multi-band WDM Coherent Transmission Systems," in Optical Fiber Communications Conference and Exhibition (OFC), 2022, paper W4I.5.
13. N. Morette, I. F. de Jauregui Ruiz and Y. Pointurier, "Leveraging ML-based QoT Tool Parameter Feeding for Accurate WDM Network Performance Prediction," in Optical Fiber Communications Conference and Exhibition (OFC), 2021, paper Th4J.4.
14. A. Ferrari, V. V. Garbhapu, D. L. Gac, I. F. de Jauregui Ruiz, G. Charlet and Y. Pointurier, "Demonstration of AI-Light: an Automation Framework to Optimize the Channel Powers Leveraging a Digital Twin," in Optical Fiber Communications Conference and Exhibition (OFC), 2022, paper M3Z.14.
15. A. Ferrari, M. Filer, K. Balasubramanian, Y. Yin, E. Le Rouzic, J. Kundrát, G. Grammel, G. Galimberti and V. Curri, "GNPy: an open source application for physical layer aware open optical networks," IEEE/OSA J. Opt. Commun. Netw. 12, C31-C40 (2020).
16. Y.R. Zhou, K. Smith, J. Weatherhead, P. Weir, A. Lord, J. Chen, W. Pan, D. Tanasoiu and S. Wu, "Demonstration of a novel technique for non-intrusive in-band OSNR derivation using flexible rate optical transponders over a live 727 km flexible grid optical link," IEEE/OSA Journal of Lightwave Technology, 35(20), pp.4399-4405, 2017.
17. E.R. Hartling, A. Pilipetskii, D. Evans, E. Mateo, M. Salsi, P. Pecci and P. Mehta, "Design, acceptance and capacity of subsea open cables," IEEE/OSA Journal of Lightwave Technology, 39(3), pp.742-756, 2021.

[i] The gain spectrum hence output power spectrum of each EDFA slightly changes during Step 2 of Fig. 1 as per-service powers are re-optimized.